

# Atom Optics Using Microfabricated Structures

C. R. Ekstrom, D. W. Keith, and D. E. Pritchard

Department of Physics and Research Laboratory of Electronics, MIT Cambridge, MA 02139, USA

Received 14 January 1992/Accepted 4 March 1992

**Abstract.** We present a novel method for fabricating precisely positioned small openings in thin silicon nitride membranes. Several optical elements for atoms have been constructed, including amplitude diffraction gratings and zone plates, and the results of experiments using these devices are presented. A method for creating a blazed diffraction grating is discussed.

**PACS:** 35.10.-d, 42.25.-p

Atom optics [1, 2] refers to two things: a new point of view in which atoms in atomic beams are thought of and manipulated like photons in light beams, and a growing collection of techniques and devices for performing this manipulation. While some demonstrations of atom optics are over 20 years old – including diffraction of atoms from crystal surfaces [3], single slit diffraction [4], and hexapole focusing lenses [5, 6] – advances in laser and nanofabrication technology have led to numerous recent demonstrations of various types of diffraction gratings [7–9] and zone plates [10, 11]. Other recent developments include the demonstration of atom mirrors using light and specially prepared surfaces [12, 13]. Recent theoretical developments suggest that momentum transfer by light offers several new possibilities for the construction of coherent beam splitters for atoms [14]. It now appears that the field of atom optics is developed well enough to allow the construction of devices containing several elements working together [15, 16].

This paper concerns optical elements for atoms made from thin membranes with precisely positioned openings for the atoms to pass through. These are essentially amplitude transmission devices – the optical analog of holes cut in black paper. The short wavelength of atomic deBroglie waves demands sub-micron size holes, requiring the use of nanofabrication techniques. Although we have used both gold and silicon nitride nanofabricated devices, here we describe only techniques for the construction of the latter. Construction of the gold gratings has been described elsewhere by its originators [17–20].

The first section of this paper describes details of the new fabrication process. The subsequent three sections discuss, in turn, the construction and performance of our atom diffraction gratings, a technique to employ electric fields to produce

blazed diffraction gratings, and results from an imaging experiment using a zone plate. We conclude by offering several speculative comments about the future of atom optics using microfabricated structures.

## 1 Fabrication

We have developed a fabrication technique to make thin (100–200 nm) silicon nitride membranes with precisely patterned holes of arbitrary shape. The membrane is stretched flat against the surface of a conventional 0.25 mm thick silicon wafer which has windows cut in it behind the patterned portions of the membrane. The pattern of holes is determined by an electron beam writer, and the overall process has been used to make patterns with minimum dimensions as small as 50 nm and overall pattern sizes up to  $3 \times 0.2$  mm. An important feature of our fabrication process is that there are few limits to the pattern that may be written on the window except those imposed by the requirement that the membrane be self-supporting. The technique has been used to construct gratings with periods from 400 to 100 nm, as well as single slits, double slits, and cylindrical zone plates. All of the construction using this method was performed at the National Nanofabrication Facility at Cornell University.

Low stress silicon nitride membranes were chosen over gold and doped silicon as a structural material for several reasons. Gold has little structural strength, which is important for the construction of large scale, uniform structures. Fabrication of doped silicon films [21] requires a poisonous and corrosive silicon etch (ethylene diamine: pyrocatechol) and silicon epitaxial growth facilities. High stress films can distort or break when they are perforated. The tensile stress

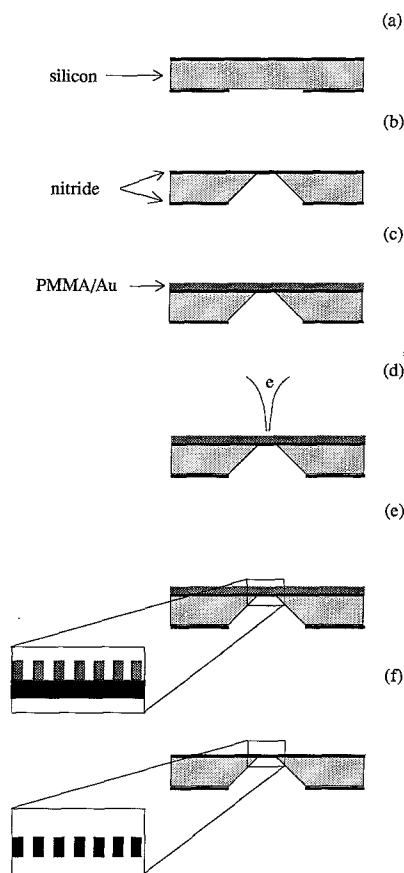


**Fig. 1a-f.** Construction steps to produce a patterned, free standing silicon nitride membrane. **a** Coat with nitride by LPCVD then pattern with photolithography and RIE. **b** We etch in hot KOH to make windows. **c** spin on PMMA then deposit Au. **d** Write pattern with 50 KeV e-beam to expose PMMA. **e** Apply gold etch then MIBK to remove the exposed PMMA (wet development). **f** RIE through the nitride, leaving the completed structure

of silicon nitride films can be reduced continuously from 1.2 GPa to less than 100 MPa by varying the growth parameters (the ratio of dichlorosilane to ammonia) of the low-pressure chemical vapor deposition (LPCVD) system [22] with some decrease in tensile strength; we used a stress of  $\sim 120$  MPa, which virtually eliminated problems of ruptures during fabrication.

The fabrication begins (Fig. 1) with the deposition of low stress silicon nitride on both sides of a double polished  $\langle 100 \rangle$  silicon wafer. The silicon nitride is deposited by low pressure chemical vapor deposition (LPCVD). A layer of standard optical photoresist is applied to what will be the back of the chip, and the pattern of windows is exposed on the wafer. After development, the nitride on the back is removed from the exposed areas of the wafer with a reactive ion etch (RIE) of  $\text{CF}_4$ .

The wafer is then immersed in hot KOH which etches each window entirely through the silicon wafer, leaving a suspended nitride *window pane* on the front of the wafer. This etch removes material with strong preference along certain crystal planes of the silicon, so the dimensions of the window on the front side of the wafer can be accurately controlled, provided the window pattern is aligned to the crystal planes of the substrate.

A 120 to 210 nm layer of Plexiglas (PMMA) is then applied to the front side of the wafer. To prevent distortions due to charging of the PMMA, a thin layer of gold is also evaporated onto the wafer. The e-beam writer (a JEOL JBX5DII) then writes the desired pattern into the PMMA. The areas in the PMMA that have been exposed by the e-beam writer have their molecular structure damaged, so they can then be washed away with a mixture of methyl isobutyl ketone (MIBK) and isopropanol (IPA). This leaves a pattern of PMMA that has not been exposed to the e-beam on the nitride window. Up to this point in the processing, all of the steps are standard, well known microfabrication techniques.

The new feature of our method is a direct process for transferring the PMMA pattern onto the nitride window. We have developed a reactive ion etch recipe [23] that etches nitride faster than PMMA, so we can use the PMMA as a mask when etching through the nitride window. Using reactive ion etching techniques is essential since wet chemical processes etch non-directionally and can also damage the structures due to forces from surface tension. The residual PMMA is then removed in an oxygen reactive ion etch.

The principal advantage of this procedure is that the pattern transfer to the membrane is performed in one step. This increases reliability, shortens processing time, and yields higher resolution. Other pattern transfer techniques, such as lift-off, which require a transfer of the pattern using a metal coating as an intermediary, are more complicated, and provide a less direct transfer of the pattern.

There are several difficulties when writing large area gratings with electron beam writing. When writing larger area gratings, it is hard to keep the grating bars parallel and the period constant over the entire area. The e-beam writer writes large area patterns by writing small fields ( $\sim 80 \mu\text{m}$  square) and then moving the sample and *stitching* them together into a large pattern. The translation stage that holds the sample is positioned by a laser interferometer to an accuracy of  $\sim 2$  nm.

In the writing process, several sources of stitching errors occur, which can be divided in two types: those that are independent and those that are dependent upon the time between when the adjacent fields were written. There are several sources of time independent stitching errors. If, for example, the sample is not mounted in the plane of motion of the translation stage, the e-beam pattern is projected onto a different plane than intended. This causes the edges of adjacent fields to be systematically misaligned and introduces periodic *noise* into the actual large scale pattern. Another source of time independent errors is due to the software correction of imperfections in the e-beam writer's electron optics. The system corrects for improper scaling, rotational misalignment, and distortions within the writing field; mis-corrections, as with sample tilt, produce periodic errors.

Field stitching errors which depend on time turn out to be much more of a problem, and appear to be due to thermal drifts during the writing process. Temperature variations can alter the distance between the reference mirrors of the position monitoring interferometer and the sample, or can distort the e-beam writer housing, moving the lenses and steering the beam. These changes will lead to errors in the final position of the e-beam relative to the sample, and will generally increase with writing time.

We have studied these two classes of errors by writing patterns of verniers across field boundaries with and without time delays. The errors which are independent of writing time are on the scale of 20 nm if care is taken in aligning the sample in the sample holder, as this reduces the amount of software correction for scaling and rotation. The thermal drifts can, however, give errors as large as 80 nm over 10 min, a typical time to write a large grating pattern. Reducing these time dependent errors then becomes a problem of minimizing the time it takes to write a grating.

To reduce the writing time, one can use higher e-beam currents or stronger e-beam resist/developer combinations, as the latter requires a lower amount of e-beam exposure for the resist to be reliably removed. Unfortunately, both approaches result in lower resolution; higher beam currents give larger spot sizes, and stronger developers don't resolve fine structures as well. Best results were obtained with 2 nA of beam current, and a 1:1 mixture of MIBK:IPA as the developer, which reduced writing times for 140 nm period gratings to approximately 2 min for a  $1.5 \times 0.05$  mm size grating.

## 2 Diffraction Gratings

One of the most interesting and versatile atom optics devices is the diffraction grating, which can serve as an atomic beam splitter or recombiner. An elegant way to realize a phase grating for atoms is by the use of a standing wave of near-resonant laser light [7]. Amplitude transmission gratings, however, have the advantages of simplicity and the ability to diffract atomic and molecular species which do not have strong laser-accessible transitions. Both types of gratings may also be used to construct a three grating interferometer [16,24].

One of the problems faced in the construction of any device using one or more diffraction gratings is the total fraction of the incident beam intensity that is transmitted. This would be maximized if the gratings could be made free standing over the entire usable beam height of several millimeters but, unfortunately, a transverse support structure has to be added to stabilize the grating bars. This support structure absorbs a significant amount of beam intensity because it covers 20% to 50% of the area of our gratings. We have found that, for a given support structure coverage, the unsupported span length of the fine grating bars should be kept as small as possible, with several microns of unsupported length being acceptable for a 50 nm wide grating bar.

The width of the slots between the grating bars as a fraction of grating period (i.e., the *open fraction*) is another important characteristic of the grating. It is possible to obtain high resolution pictures of fabricated gratings with a scanning electron microscope, but we have found that these pictures do not always correspond to how the gratings *look* to the atomic beam; we have occasionally found gold gratings which looked good in the electron microscope but were *opaque* to atoms (these gold gratings were not metal coated before inspection, so the SEM may not have seen material in the slots). The best diagnostic that we have to investigate the open fraction seen by the atoms is the atomic diffraction pattern itself. Figure 2 shows diffraction patterns produced

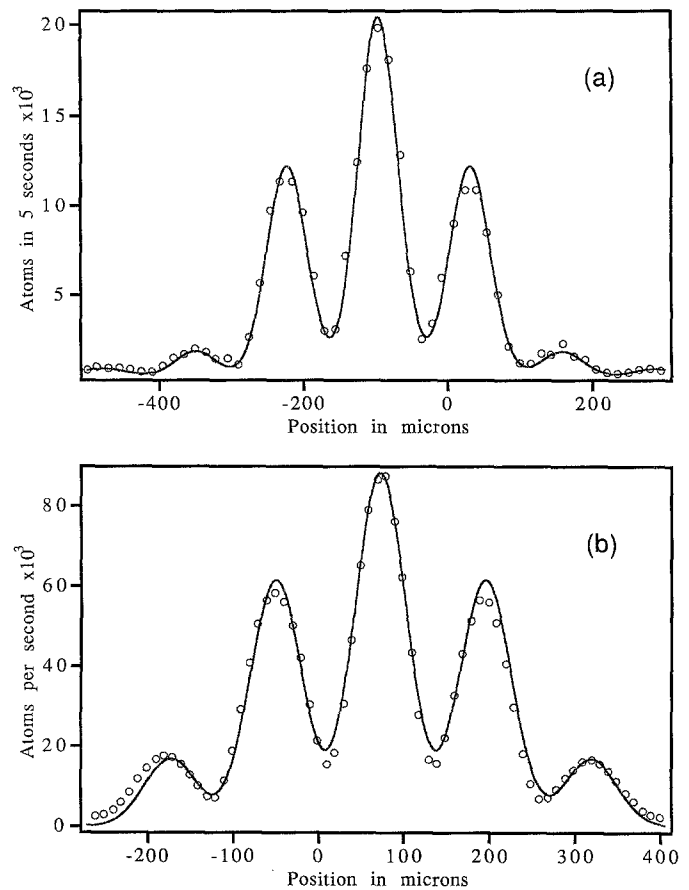


**Fig. 2a, b.** Diffraction of an atomic beam from a free standing 200 nm period diffraction grating. The data in **a** was taken with a gold grating built at the MIT Submicron Structure Lab. The theoretical fit is for an open fraction of 39%. The data in **b** was taken with a silicon nitride grating constructed at the National Nanofabrication Facility at Cornell University. The fit is for an open fraction of 33%

by 200 nm period gratings built with different methods and having different open fractions. The diffracted sodium beam has a deBroglie wavelength of 16 pm. The open fraction of the diffraction gratings seen by the atoms determines the relative heights of the diffracted orders, as the modulation of the intensity in each order is given by the single slit pattern formed by each slot between grating bars.

The fits shown in Fig. 2 convolve the theoretical diffraction pattern and an instrumental profile that is determined by a gaussian fit to the zero order diffraction peak. The relative heights of the various diffracted orders are thus determined by one variable, the open fraction of the grating. Although adjustment of the open fraction value gives a clear best fit with only  $\sim 1\%$  uncertainty in the value, it is not possible to fit the diffraction data to within experimental error. Additional averaging in the fit due to the 12% velocity width of our atomic beam does not significantly reduce the strong disagreement in the heights of orders that we predict to be strongly suppressed using the best fit to the open fraction. The most likely source of this disagreement is due to small variations in the size and placement of the actual openings in the grating; this noise causes the opening to vary from the average size (which would produce essentially zero amplitude in the strongly suppressed order). We feel that the

open fraction that we get from the fitting process represents a good *mean open fraction* value for the grating.

### 3 Blazed Gratings

In addition to varying the open fraction of the grating, the intensity in the various diffracted orders could be selectively increased by using blazed gratings. In classical optics, the intensity of the various diffracted orders produced by a blazed diffraction grating is tailored by systematically varying the plate thickness so that the phase of the transmitted wave varies across each grating element. Analogously, to make a blazed grating for atoms, we need to vary the phase of the atomic wave function over the opening between grating bars.

We propose to create this phase shift by applying electric fields that vary in magnitude over the width of the slots in the diffraction grating. These electric fields could be created by metallizing the front and back of the grating and then applying a voltage between the metal electrodes (Fig. 3). The electric field in the slots causes energy shifts in the atoms (the dc Stark shift). The potential ( $U$ ) is much smaller than the incident energy ( $E$ ) of the atoms ( $U/E = 10^{-3}-10^{-4}$ ), so an eikonal approximation [25] can be used to calculate the phase shift given to an atom traveling through the slot in the  $z$  direction a distance  $x$  from the center. In this approximation

$$\phi(x) = \int_x \mathbf{k} dz - \int_x \mathbf{k}_0 dz \approx \frac{1}{\hbar v_0} \int_x U(x, z) dz,$$

where  $v_0$  is the incident atomic velocity, and  $\mathbf{k}_0$  is the  $\mathbf{k}$  vector of the atoms when  $U = 0$ . Focusing or defocusing of the atoms (i.e., blazing of the grating) results because  $\phi$  depends on  $x$ .

We have calculated the effects of such a blazing potential for a 200 nm thick grating on a sodium beam with a deBroglie wavelength of 16 pm. The phase shift across the slot  $\phi(x)$  fits a parabola to within 4%, except for  $\sim 1/12$  of the slot width closest to either slot edge (near the electrodes). The use of a parabolic functional form in our calculations was motivated by the desire for a simple form that would fit the data and allow an analytic solution of the single slit integral. We calculated the single slit diffraction pattern analytically for one such slot, allowing for the spatially varying phase shift (the fitted parabola), as a function of the applied voltage. This modified single slit pattern then is used a form factor to determine the intensities in the various diffracted orders. The results of our calculations appear in Fig. 4, where we show the intensities in various diffracted orders as a function of applied voltage. Because the phase shift is symmetric about the center of the slot, the positive and negative diffracted orders have the same intensities.

An advantage of blazing is that it allows the use of wider slots for a given grating period, because the intensity in the diffraction pattern can be tuned with the applied voltage as intensity normally sent to the zero order is diffracted into higher orders. This results in more total transmitted intensity due to the lower overall opacity of the gratings, well as the larger intensities in the higher orders. This can be seen

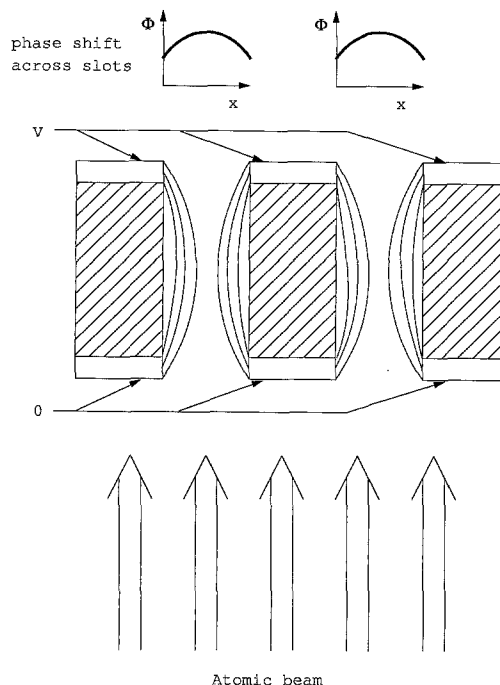


**Fig. 3.** Cross section of several grating bars of a blazed atom grating. Hatched areas are silicon nitride. The potential difference ( $V$ ) to produce the electric fields is applied between the front and the back electrodes. The electric field lines, shown between the grating bars, lead to varying phase shifts at different positions across each slot (insets)

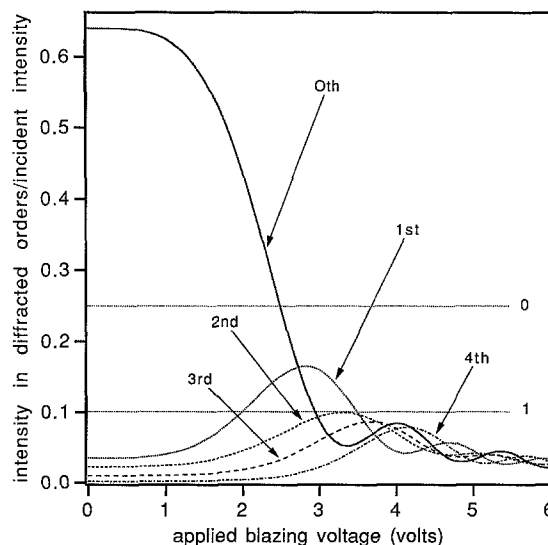


**Fig. 4.** Predicted intensity in various orders of our sodium beam diffracting through a 200 nm thick blazed grating with an open fraction of 80%. The horizontal axis represents the voltage applied between the front and the back of the grating. The two horizontal dotted lines represent the intensities of the zero and first order maxima (labeled by 0 and 1 respectively) of an unaltered 50% open grating

in Fig. 4, where the first order diffraction of the 80% open grating at a blazing voltage of 2.8 V is approximately 1.6 times that of an unaltered 50% open grating. Intensities in higher orders can be increased even more dramatically. For example, the second order diffraction of the 80% open grating at 3.3 V is almost as large as the first order diffraction in

the unaltered 50% grating (which has the largest first order peak of any unblazed grating).

#### 4 Zone Plates

Zone plates for atoms have been constructed [10, 11, 21], demonstrated [10], and studied [11] by several groups. Both spherical [11, 21] and cylindrical [10] zone plates have been built. We give here a discussion of our experimental results first presented elsewhere [10]. The objective of the experiment was to image an aperture (one of our collimation slits) onto our detector using a cylindrical zone plate. The atomic beam was a seeded supersonic nozzle beam of sodium in an argon carrier gas. The expansion of the carrier gas gave the beam of sodium a narrow velocity distribution ( $\Delta v/v = 12\%$ ), and a wavelength of 16 pm. The beam illuminated a 20  $\mu\text{m}$  wide collimation slit (Fig. 5). A cylindrical zone plate (130  $\mu\text{m}$  wide by 500  $\mu\text{m}$  tall) was placed 1.5 m after the slit, and imaged the slit onto the detector plane, located 0.9 m downstream. The sodium atoms were detected after they surface ionized on a moveable 25  $\mu\text{m}$  hot wire.

We have performed a complete numerical simulation of the performance of our zone plate using a procedure which has been described in detail elsewhere [26, 27]. Briefly, we calculate the sum of amplitudes at the detector plane generated by a point of the illuminated collimation slit passing through all the open parts of the zone plate, then sum the intensities for different locations in the slit and over a distribution of velocities.

The result of this simulation appears in Fig. 6, together with the experimental results. The curves were adjusted by using only the mean position and total intensity of the experimental and calculated images. The experiment was not set up in a way to make it possible to get an accurate figure for the amount of incident intensity in the image. The experimental results show a clear central peak, indicative of considerable focusing by the zone plate. The measured image, however, has more smoothing and greater width than calculated. There are several factors that could artificially enhance the observed image width. A narrowing of all open areas by a constant amount would cause the intensity of the zero order pedestal to fall off roughly as the inverse of the distance from the center of the image (but would not appreciably widen the central peak). A narrowing of this type large enough to account for the almost total suppression of intensity at the edge of the zero order pedestal is larger than we feel is reasonable to attribute to the fabrication process. A slight bend or tilt in the detector wire could also broaden the predicted sharp edges.

One thing that is obvious from the simulation of the cylindrical zone plate lens is that an unblazed amplitude zone plate is a very inefficient piece of atom optics, making an image containing only about 11% of the intensity of the image formed by an ideal lens. Thus, in our experiment, the pattern expected from a non focusing aperture with the same width as the zone plate exceeds the peak intensity expected with the zone plate in place (see Fig. 6). This intensity loss would seem to rule out the practical use of zone plate lenses except in a few special applications (e.g., to make an achromatic atom lens [2] or an atom microscope).

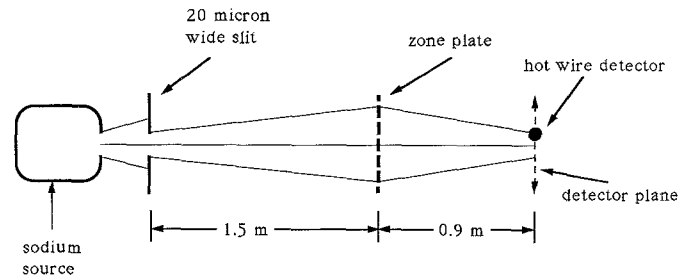


**Fig. 5.** Experimental setup used for imaging a 20  $\mu\text{m}$  wide slit onto our hot wire detector using a cylindrical zone plate

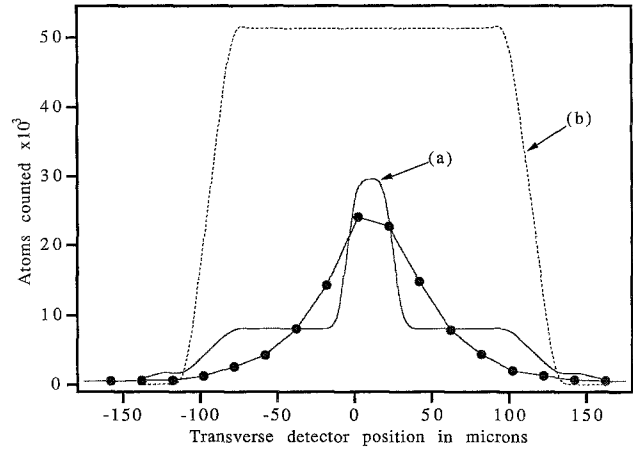


**Fig. 6.** Experimental data (points) showing the image formed by a zone plate lens (the line joining the points is solely to guide the eye). Curve *a* is the theoretically predicted pattern formed by the lens (assuming a 1/2 density support structure), and *b* is the pattern predicted if the zone plate is replaced by a slit of identical size. The curves were adjusted by using only the mean position and total intensity of the experimental and calculated images

The performance of an amplitude zone plate is determined almost entirely by the size of the smallest feature  $s$  (the size of the slots or bars at its outer edge): This determines the maximum first order diffraction angle for a deBroglie wavelength  $\lambda_{dB}$ , of  $\theta_m = \lambda_{dB}/2s$ , and directly determines the  $f$ -number,  $f = 1/2\theta_m = s/\lambda_{dB}$ . The focal spot size is  $\lambda_{dB}f \cong s$ , so it is not improved (unlike the  $f$  number) by using a slow atomic beam (we have assumed  $s \ll \lambda_{dB}$ ). The maximum transverse momentum transfer of the lens is  $p_{\perp} = h/2s$ , corresponding to a maximum transverse temperature that can be focused [28] of  $p_{\perp}^2/2m$  ( $\sim 42 \mu\text{K}$  for sodium atoms, assuming  $s = 50 \text{ nm}$ ).

#### 5 Future Directions

There are several promising areas to explore with fabricated amplitude structures for atom optics. These include better diffraction gratings with smaller periods and larger areas, blazed diffraction gratings, and more general atom holograms.

We have recently completed an attempt to construct fine period, large area diffraction gratings for our atom interferometer experiments. We have constructed grating periods as small as 100 nm that have  $\sim 35 \text{ nm}$  free standing bars. To

write smaller periods at more reasonable grating open fractions will require less e-beam current to get a smaller spot size. Since this will increase the writing time, thermal drifts in the e-beam writer will become a severe problem. Perhaps moving to a field emission version of the e-beam writer or a return to optical holographically written gratings using UV light [17–29] will be necessary to make uniform large area gratings with fine periods.

As the far field diffraction patterns produced by gratings, single slits, and double slits are simply the Fourier transform of the pattern itself, there is no reason not to tailor the e-beam written pattern to make more complicated images in the far field (or indeed in the intermediate field). With the addition of lenses and slow, bright atomic beams, one has all of the tools to do holographic atom printing onto a substrate [30]. This would be analogous to reduction printing in standard photolithography. With the rapidly growing collection of atom optics elements, atom beam experiments may soon be used even in the construction of micro-structures.

*Acknowledgements.* We would like to thank Mark Shattenburg and Hank Smith for introducing us to the opportunities and intricacies of nanofabrication, and to acknowledge the discussions and help in the lab from the staff at NNF, Mike Rooks and Bob Soave in particular. We would also like to thank Alex Martin for careful and valuable readings of this manuscript. This work was supported by ARO grant DAAL03-89-K-0082, ONR grant N00014-89-J-1207, and JSEP grant DAAL03-89-C-0001.

## References

1. V.I. Balykin, V.S. Letokov: *Phys. Today* (1989)
2. D.E. Pritchard: *Atom Optics*, ed. by J.C. Zorn, R.R. Lewis, ICAP 12 (American Institute of Physics, Ann Arbor 1991) pp. 165–174
3. I. Estermann, O. Stern: *Z. Phys.* **61**, 95 (1930)
4. J.A. Leavitt, F.A. Bills: *Am. J. Phys.* **37**, 907 (1969)
5. H. Friedburg, W. Paul: *Z. Phys.* **130**, 493 (1951)
6. H. Friedburg, W. Paul: *Naturwissenschaften* **38**, 159 (1951)
7. P.L. Gould, G.A. Ruff, D.E. Pritchard: *Phys. Rev. Lett.* **56**, 827 (1986)
8. D.W. Keith, M.L. Shattenburg, H.I. Smith, D.E. Pritchard: *Phys. Rev. Lett.* **61**, 1580–1583 (1988)
9. O. Carnal, A. Faulstich, J. Mlynek: *Appl. Phys. B* **53**, 88 (1991)  
The microstructures used in this work and in references 11 and 15 were constructed by Heidenhain, Inc. (Traunreut, Germany)
10. D.W. Keith, M.J. Rooks: *J. Vac. Sci. Technol. B* **9**, 2846 (Nov/Dec 1991)
11. O. Carnal, M. Sigel, T. Sleator, H. Takuma, J. Mlynek: *Phys. Rev. Lett.* **67**, 3231 (1991)
12. J.J. Berkhout, O.J. Luiten, I.D. Setija, T.W. Hijmans, T. Mizusaki, J.T.M. Walraven: *Phys. Rev. Lett.* **63**, 1689–1692 (1989)
13. R.B. Doak: *Opt. Soc. of Am. Tech. Digest* **15**, 250 (1989)
14. Personal Communication with P. Meystre
15. O. Carnal, J. Mlynek: *Phys. Rev. Lett.* **66**, 2689 (1991)
16. D.W. Keith, C.R. Ekstrom, Q.A. Turchette, D.E. Pritchard: *Phys. Rev. Lett.* **66**, 2693 (1991)
17. E.H. Anderson, C.M. Horowitz, H.I. Smith: *Appl. Phys. Lett.* **43**, 874 (1983)
18. N.M. Ceglio, A.M. Hawryluk, R.H. Price: *Proc. SPIE Int. Soc. Opt. Eng.* **316**, 134 (1981)
19. A.M. Hawryluk, N.M. Ceglio, R.H. Price, J. Melngailis, H.I. Smith: *J. Vac. Sci. Technol.* **19**, 897 (1981)
20. H.I. Smith, E.H. Anderson, A.M. Hawryluk, M.L. Shattenburg: In *X-Ray Microscopy*, ed. by G. Schmahl, D. Rudolph, Springer Ser. Opt. Sci., Vol. **43** (Springer, Berlin, Heidelberg 1983)
21. D.M. Tennant, J.E. Bjorkholm, M.L. O'Malley, M.M. Becker, J.A. Gregus, R.W. Epworth: *J. Vac. Sci. Technol. B* **8**, 1975 (1990)
22. Personal communication with M. Rooks and B. Soave
23. The RIE recipe is 42 sccm CF<sub>4</sub> and 5 sccm H<sub>2</sub> at 15 mTorr with 100 W of rf power, yielding 340 V of dc bias
24. V.P. Chebotayev, B.Y. Dubetsky, A.P. Kasantsev, V.P. Yakovlev: *J. Opt. Soc. Am. B* **2**, 1791 (1985)
25. L.D. Landau, E.M. Lifshitz: In *Quantum Mechanics (Nonrelativistic theory)*, Vol. 3 (Pergamon, New York 1977) pp. 538
26. Q.A. Turchette, D.E. Pritchard, D.W. Keith: Submitted to *J. Opt. Soc. Am.* (1991)
27. Q.A. Turchette: S.B., Thesis MIT (1991)
28. This value is incorrectly given as 20  $\mu$ K in Ref. 2
29. Personal communication with H.I. Smith, S.C. Hector, M.L. Shattenburg, and E.H. Anderson
30. Sodium gratings on silicon substrates have been produced by M. Prentiss et al.